

Synthesis and characterisation of novel multidentate ferrocene ligands and their Re(I) and Pt(II) complexes

Karen Bushell^{a,1}, Constantina Gialou^a, Chay Hian Goh^a, Nicholas J. Long^{a,*}, Jeff Martin^a, Andrew J.P. White^a, Charlotte K. Williams^a, David J. Williams^a, Marco Fontani^b, Piero Zanello^b

^a Department of Chemistry, Imperial College of Science, Technology and Medicine, South Kensington, London SW 7 2AY, UK

^b Dipartimento di Chimica, dell'Università di Siena, Via Aldo Moro, 53100 Siena, Italy

Received 19 January 2001; received in revised form 25 June 2001; accepted 26 June 2001

Abstract

Two new multiply methylthio-substituted ferrocene ligands 1,1',2-tris- and 1,1',2,2'-tetrakis-(methylthio)ferrocene (TriMSF and TMSF, respectively), have been prepared by a simple, single-step procedure. Adjacent substitution of the cyclopentadienyl rings leads to potentially versatile multidentate ligands. The coordination chemistry of these ligands has been explored by reaction with labile Re(I) and Pt(II) metal centres to give complexes **1–4**, featuring binding of one or two metal centres. The complexes have been characterised by ¹H-NMR and infrared spectroscopies, mass spectrometry and microanalysis. The solid state structures of **1** and **3** have been determined, and show distorted octahedral environments about rhenium and out-of-plane folds of the five-membered chelate rings within the structures. The ligands TriMSF and TMSF exhibit the expected reversible one-electron oxidation of ferrocene molecules. The coordination of thioether substituents to the rhenium or to the platinum centres has a strong electronic impact on the redox ability of the respective complexes, resulting in ferrocene oxidation being more difficult by about 0.3–0.5 V, but it does not compromise the chemical reversibility of the respective ferrocene/ferrocenium redox changes. © 2001 Published by Elsevier Science B.V.

Keywords: Rhenium; Platinum; Thioether; Chelate; Redox

1. Introduction

To date, there have been very few examples of multiple substitution of the ferrocene ring to incorporate more than two donor heteroatoms, and those that are known generally feature nitrogen or phosphorus atoms [1,2]. With three, four or even five heterodonor atoms substituted onto the ferrocene unit, many new bonding possibilities arise. In a recent paper [3], six main classes of ferrocene-based phosphine ligands were identified and arranged on the basis of their ferrocene ring substitution pattern (e.g. monophosphines, diphosphines

(1,1'-, 1,2- or 1,3-disubstitution), triphosphines and oligophosphines). Some of these systems have been more extensively studied than others, primarily due to difficulties in the synthesis and purification of the multiply-substituted ferrocenes. However, in recent years, elegant syntheses by, in particular, the groups of Butler [4], Broussier [5] and Balavoine [6] have opened up the area. We have long had an interest in chalcogen-substituted ligands, and recently communicated the synthesis of multiply-substituted SMe ferrocenyl derivatives [7] and the catalytic potential of transition metal complexes based on these and related ligands [8]. This manuscript features the full synthetic discussion of two multidentate methylthio-substituted ferrocenes, 1,1',2-tris(methylthio)ferrocene (TriMSF) and 1,1',2,2'-tetrakis(methylthio)ferrocene (TMSF), and their versatility as ligands is demonstrated by the synthesis and characterisation of several rhenium(I) and platinum(II) complexes.

* Corresponding author. Tel.: +44-207-594-5781; fax: +44-207-594-5804.

E-mail address: n.long@ic.ac.uk (N.J. Long).

¹ Work carried out at the Department of Chemistry, University of Cambridge.

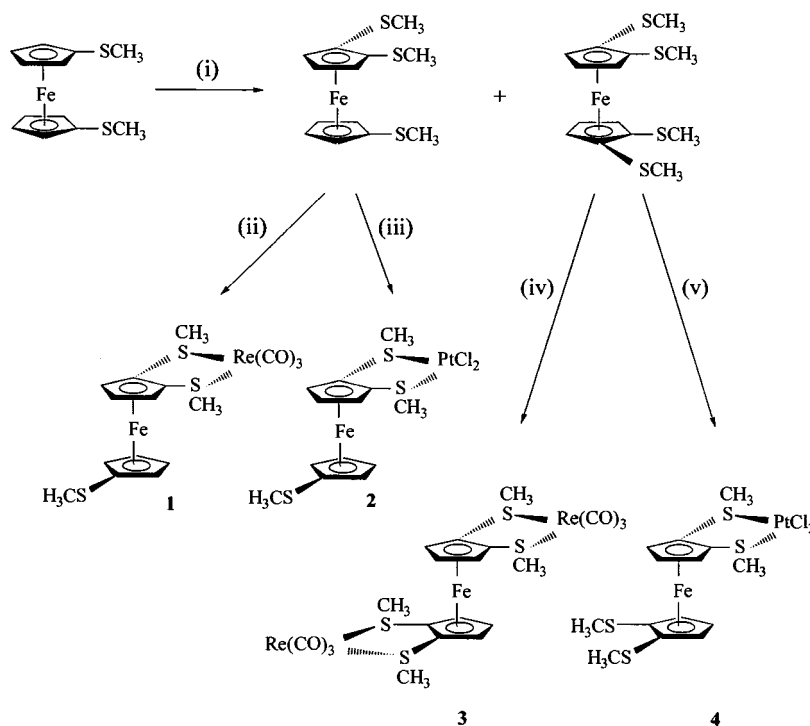
2. Results and Discussion

The ligands TriMSF and TMSF were prepared by lithiation of 1,1'-bis(methylthio)ferrocene (BMSF) using *tert*-butyllithium in hexane, followed by addition of dimethyldisulphide. The foul-smelling oily, orange-brown products were separated from BMSF and other highly-substituted ferrocenes via column chromatography on neutral grade II alumina using mixtures of petroleum ether (40–60) and diethylether (10:1 to elute TriMSF and 5:1 to elute TMSF). TMSF could be obtained as a low-melting orange-brown crystalline solid, if left to stand coupled with rigorous removal of solvent, whilst TriMSF was isolated as a brown oil. Use of *tert*-butyllithium as opposed to *n*-butyllithium was favoured for better yields and easier separation of products and by-products.

The splitting patterns observed in the $^1\text{H-NMR}$ spectra of the ligands indicate the arrangement of the substituted methylthio groups, with two adjacent to each other on one C_5 ring and one on the other in TriMSF and two adjacent groups on each C_5 ring in TMSF. There are two inequivalent methylthio signals for TriMSF, resulting from the two equal methylthio groups on the same C_5 ring (at lower field) and the methylthio group on the other C_5 ring. The expected three sets of triplets (two 'pseudo' ones for $\text{H}_{2,5}$ and $\text{H}_{3,4}$ of the mono-substituted ring and one for the proton *meta* to the substituents of the di-substituted

ring) and a doublet are observed for the C_5 ring protons. For TMSF, a doublet at lower field is assigned to the two equivalent C_5 ring protons *ortho* to the methylthio substituents, whilst a triplet at higher field is due to the proton *meta* to the substituents. By symmetry, all four methylthio substituents are equivalent and a singlet is observed for the methyl protons.

To explore the binding properties of these ligands, they were reacted with labile Re(I) and Pt(II) metal centres (Scheme 1). Bidentate coordination was expected from the ligands and it was of interest to elucidate the position of binding (i.e. between the sulphur atoms on the same C_5 ring or between one sulphur on one ring and one on another) and the number of metal centres that could be coordinated. Complex **1** was formed by reacting TriMSF and $\text{Re}(\text{CO})_5\text{Br}$ in refluxing THF and the reaction was monitored by IR spectroscopy via the changes in the carbonyl stretching region. Strong bands at 2037, 1948, 1906 cm^{-1} were observed, a pattern typical of a *fac*- $\text{Re}(\text{CO})_3\text{Br}(\text{L-L})$ arrangement [9]. In this case, bidentate coordination can occur in two ways as stated above (Fig. 1), and the preferred mode can be elucidated by $^1\text{H-NMR}$ spectroscopy. Were the binding to occur using one sulphur on one ring and one on another, all three methylthio groups would be inequivalent. If the binding is between the two sulphur atoms on the same ring, only two different methylthio signals (intensity 2:1) would be expected. Signals due to this latter conformation are



Scheme 1. The syntheses of TriMSF, TMSF and complexes **1**–**4**. (i) *t*-BuLi, hexane, 16 h; Me_2S_2 , 4 h; (ii) $\text{Re}(\text{CO})_5\text{Br}$ (one equivalent), THF, Δ , 10 h; (iii) *cis*- $\text{PtCl}_2(\text{NCPh})_2$ (one equivalent), toluene, 90 °C, 15 h; (iv) $\text{Re}(\text{CO})_5\text{Br}$ (two equivalents), THF, Δ , 10 h; (v) *cis*- $\text{PtCl}_2(\text{NCPh})_2$ (one equivalent), toluene, 90 °C, 15 h.

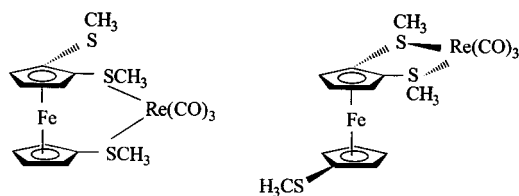


Fig. 1. Possible coordination structures for **1**.

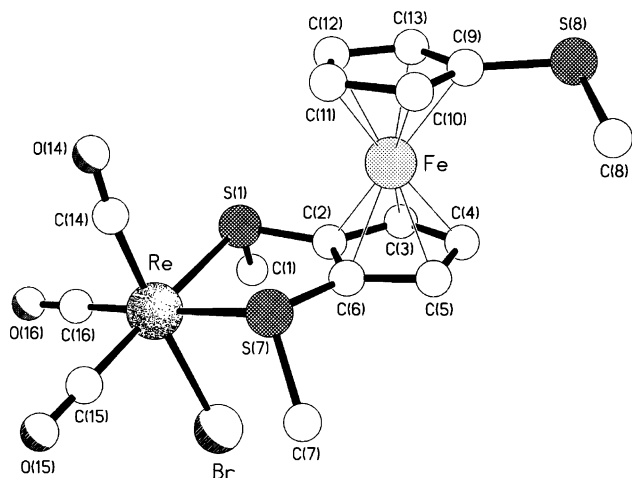


Fig. 2. The molecular structure of **1** (major occupancy isomer).

indeed those observed (and this binding mode has also been found in our studies with $W(CO)_4$ centres [7]). However, there are actually three pairs of singlets of 2:1 intensity in this region, which implies the presence of three different species. A possible explanation for this would be the existence of invertomers in solution due to sulphur inversion of the substituents on the ligands and reversal of the S–M–S portion of the chelate rings. This type of fluxionality has been observed in similar ligand types [9–11] and occurs when the rate of the fluxional processes are slow enough for the possible invertomers to be distinguished by NMR experiments at low to ambient temperatures. Further detailed variable temperature NMR spectroscopy measurements are necessary to elucidate the exact nature of the process but it has been established in analogous species that invertomers are likely to be *meso* forms (i.e. when the methyl groups on the sulphur atoms are oriented in a *syn* fashion) or *DL* forms (where the groups are *anti* to each other). The relative invertomer populations are known to be a function of a sensitive balance of factors such as the nature of the metal, substituents, coordinated ligands, solvent and temperature. It is interesting to note that in the solid state, the methyl substituents on the sulphurs bound to the metal are always oriented *syn* (or in the *meso* form) (vide supra). The binding mode was confirmed by a structural determination of **1**. The X-ray analysis reveals a structure very similar to that of the closely related tungsten tetracarbonyl ana-

logue [7], though with some notable differences. In the present structure (Fig. 2), there is disorder with the positions of the axial carbonyl and bromide substituents being reversed in 20% of the molecules in the crystal; the following discussion will relate to the major occupancy (80%) structure. The geometry at rhenium is distorted octahedral with *cis* angles in the range 85.35(9) to 93.8(4)°, the most acute angle being associated with the bite of the TriMSF ligand. The Re–S distances are unexceptional at 2.511(3) and 2.500(3) Å to S(1) and S(7), respectively (Table 1). The five-membered chelate ring has a pronounced (ca. 21°) out of plane fold about the S(1)⋯S(7) vector, thereby projecting the bromine atom into the cleft formed between the two SMe substituents. It is interesting to note that this fold is in the opposite sense to that observed in the related tungsten species [7] (where the fold is ca. 12°). A consequence of these different ‘folds’ is a significant difference in the C(1)⋯C(7) separations in the two structures, being 5.65 Å in the rhenium complex but only 4.42 Å in the tungsten species. Similarly, the internuclear Re⋯Fe separation is increased to 4.72 Å, cf. 4.54 Å for tungsten. The pyramidalisations at the two sulphur centres are essentially the same, both here and in the tungsten complex; the sums of the angles at sulphur being 311.3 and 314.2° in the rhenium complex, cf. 312.1 and 312.9° in the tungsten compound. Another difference between the two structures is in the degree of stagger of the pairs of ferrocenyl C₅ rings; in the tungsten species the two C₅ rings are eclipsed, whereas in the present structure there is a ca. 13° stagger and the rings are inclined by ca. 3°. In both structures the S(8)–Me bond is rotated by ca. 24° out of its associated C₅ ring plane. There are no intermolecular interactions of note.

Complex **2** was formed from the reaction of TriMSF (slight excess) and *cis*-PtCl₂(NPh)₂ in refluxing toluene. The crude solid was washed with hot hexane and diethylether to remove any traces of unreacted ligand. The square planar Pt(II) centre is confirmed to bind to

Table 1
Selected bond lengths (Å) and bond angles (°) for **1**

Bond lengths			
Re–Br	2.624(2)	Re–S(1)	2.511(3)
Re–S(7)	2.500(3)	Re–C(14)	1.9299(12)
Re–C(15)	1.946(12)	Re–C(16)	1.89(2)
Bond angles			
S(1)–Re–Br	88.92(8)	S(7)–Re–Br	88.57(7)
S(7)–Re–S(1)	85.35(9)	C(14)–Re–Br	176.4(4)
C(15)–Re–Br	90.3(4)	C(16)–Re–Br	93.0(4)
C(14)–Re–S(1)	89.5(5)	C(15)–Re–S(1)	178.4(4)
C(16)–Re–S(1)	93.8(4)	C(14)–Re–S(7)	88.1(5)
C(15)–Re–S(7)	93.2(4)	C(16)–Re–S(7)	178.2(4)
C(14)–Re–C(15)	91.2(6)	C(16)–Re–C(14)	90.3(6)
C(16)–Re–C(15)	87.7(5)		

the ligand via the same coordination mode as in **1** (i.e. through the two sulphurs on the same ring) from $^1\text{H-NMR}$ spectroscopy. Two methylthio signals are observed in a ratio of 2:1, with the higher intensity signal also featuring platinum satellites ($J_{\text{Pt-H}} = 23.0$ Hz) and there is a large downfield shift of these signals compared to the relevant signals in the free ligand. This shift has been attributed to the magnetic anisotropy or the inductive effect of the platinum centre [12]. The expected set of signals for the Cp ring proton region

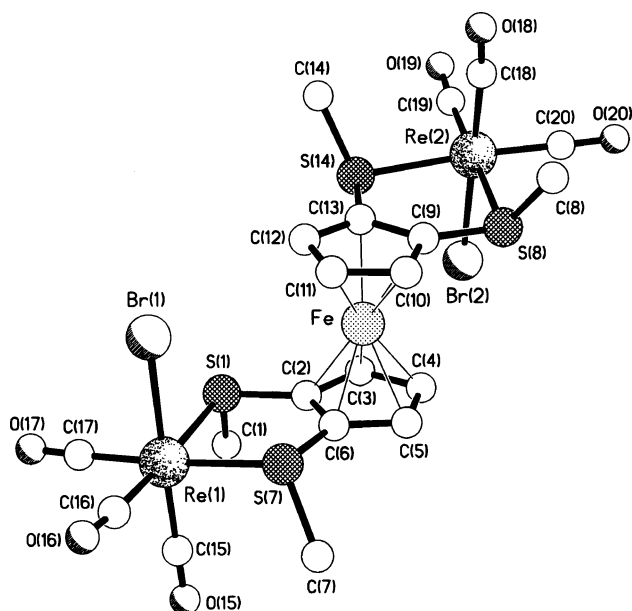


Fig. 3. The molecular structure of **3** (major occupancy isomer).

Table 2
Selected bond lengths (Å) and bond angles (°) for **3**

Bond lengths			
Re(1)–Br(1)	2.606(2)	Re(1)–S(1)	2.498(3)
Re(1)–S(7)	2.512(3)	Re(1)–C(15)	1.93(2)
Re(1)–C(16)	1.93(2)	Re(1)–C(17)	1.91(2)
Re(2)–Br(2)	2.596(4)	Re(2)–S(8)	2.490(4)
Re(2)–S(14)	2.515(3)	Re(2)–C(18)	1.92(2)
Re(2)–C(19)	1.94(2)	Re(2)–C(20)	1.90(2)
Bond angles			
S(1)–Re(1)–Br(1)	83.15(9)	S(7)–Re(1)–Br(1)	84.41(9)
S(1)–Re(1)–S(7)	85.83(10)	C(15)–Re(1)–Br(1)	178.7(4)
C(16)–Re(1)–Br(1)	91.5(5)	C(17)–Re(1)–Br(1)	92.7(4)
C(15)–Re(1)–S(1)	96.4(5)	C(16)–Re(1)–S(1)	174.6(5)
C(17)–Re(1)–S(1)	91.8(5)	C(15)–Re(1)–S(7)	94.4(4)
C(16)–Re(1)–S(7)	93.4(4)	C(17)–Re(1)–S(7)	176.4(4)
C(15)–Re(1)–C(16)	88.9(7)	C(17)–Re(1)–C(15)	88.5(6)
C(17)–Re(1)–C(16)	88.7(7)	S(8)–Re(2)–Br(2)	85.57(12)
S(14)–Re(2)–Br(2)	84.22(11)	S(8)–Re(2)–S(14)	85.91(11)
C(18)–Re(2)–Br(2)	176.9(10)	C(19)–Re(2)–Br(2)	95.5(7)
C(20)–Re(2)–Br(2)	91.9(6)	C(18)–Re(2)–S(8)	91.4(10)
C(19)–Re(2)–S(8)	178.5(6)	C(20)–Re(2)–S(8)	93.0(7)
C(18)–Re(2)–S(14)	94.9(9)	C(19)–Re(2)–S(14)	93.2(5)
C(20)–Re(2)–S(14)	176.0(6)	C(18)–Re(2)–C(19)	87.5(12)
C(20)–Re(2)–C(18)	89.0(11)	C(20)–Re(2)–C(19)	88.0(8)

were observed, namely, two pseudo triplets of the C_5H_4 ring and a doublet and triplet for the C_5H_3 ring. However, there is no evidence for the presence of invertomers—the quoted signals being sharp with no minor, less intense signals observed. This is in contrast with the NMR spectra seen for **1**, and indicates that in **2** the sulphur inversion fluxionality is not compatible with the NMR timescale or that only one invertomer (a *meso* form) is found in solution.

In order to probe the possibility of coordination of two metal centres to the novel ligands to form a trimetallic complex, TMSF was reacted with two equivalents of $\text{Re}(\text{CO})_5\text{Br}$. An analogous procedure was used to that for the formation of **1**, and similar IR data were obtained. Though again complicated by the presence of invertomers, the $^1\text{H-NMR}$ spectrum indicated that two metal centres were indeed coordinated via the bonding mode observed previously (i.e. coordination to sulphurs on the same C_5 ring). The predicted simple (due to the symmetry of the complex) splitting pattern, of one methylthio signal and two C_5 ring proton signals, was observed, along with less intense signals due to solution invertomers. The X-ray structure of the dimeric complex **3** is illustrated in Fig. 3. As was the case in **1**, there is disorder (70:30) in one of the pairs of axial carbonyl/bromide substituents—that associated with Re(2); only the major occupancy form will be discussed. Although the structure has the potential to have inversion symmetry, this has not been utilised, the two C_5 rings being virtually eclipsed with a consequent proximal relationship between S(1) and S(14) [and distal between S(7) and S(8)]. As in **1**, in the solid state the pairs of S–Me substituents are, in both cases, *syn* (vide infra). The out of plane folds in the two chelate rings are both in the same sense but opposite to that seen in **1**, and the magnitude of the fold angles are noticeably reduced [ca. 9° for Re(1) and ca. 11° for Re(2)]. The associated $\text{C}(1)\cdots\text{C}(7)$ and $\text{C}(8)\cdots\text{C}(14)$ separations are 5.16 and 5.27 Å respectively, and the non-bonded $\text{Fe}\cdots\text{Re}$ distances are 4.70 Å to Re(1) and 4.69 Å to Re(2). The geometries at the two rhenium centres are distorted octahedral with *cis* angles in the range 83.15(9) to 96.4(5) $^\circ$ at Re(1) and 84.22(11) to 95.5(7) $^\circ$ at Re(2); the chelate bite angles are 85.83(10) and 85.91(11) $^\circ$ at Re(1) and Re(2) respectively (Table 2). The Re–S distances do not differ noticeably from those in **1**, being in the range 2.490(4) to 2.515(3) Å. There are no noteworthy intermolecular interactions.

As a contrast to bimetallic coordination with TMSF, monometallic coordination was carried out in the formation of **4**. TMSF and *cis*- $\text{PtCl}_2(\text{NPh})_2$ were refluxed in toluene in equimolar quantities to form, after work-up, an orange–brown solid. Similar spectroscopic observations were seen as for complex **2**, with two equal intensity methylthio resonances, one shifted downfield and possessing ^{195}Pt satellites ($^3J_{\text{Pt-H}} = 23.5$

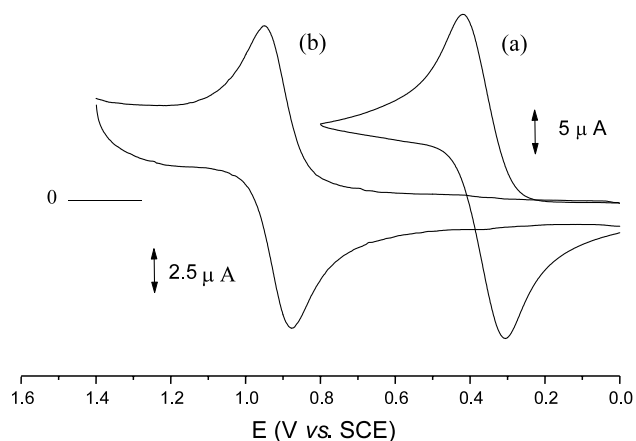


Fig. 4. Cyclic voltammetric responses recorded at a platinum electrode on CH_2Cl_2 solutions containing $[\text{NBu}_4][\text{PF}_6]$ (0.2 mol dm^{-3}) and: (a) TriMSF ($1.6 \times 10^{-3} \text{ mol dm}^{-3}$); (b) **2** ($1.1 \times 10^{-3} \text{ mol dm}^{-3}$). Scan rate 0.2 V s^{-1} .

Hz) and two sets of doublets and triplets due to the different C_5 ring protons. As with **2**, there was no evidence for invertomer formation.

3. Electrochemistry

As a typical example of the redox effects of coordination of metal fragments to the thioether substituents of the present ferrocene ligands, Fig. 4 compares the cyclic voltammetric responses of TriMSF (a) with that of the corresponding platinum complex **2** (b). Both the derivatives exhibit an oxidation process displaying features of chemical reversibility within the cyclic voltammetric time scale. In each case, controlled potential coulometry showed the consumption of one electron per molecule. In confirmation of the complete chemical reversibility of such anodic steps, which are confidently assigned to the respective ferrocene/ferrocenium processes, cyclic voltammetry on the exhaustively oxidised solutions displays voltammetric profiles quite comple-

mentary to the original ones. Upon exhaustive one-electron oxidation, the yellow solutions of TriMSF and **2** turn brown–green and brown, respectively. If one considers that iron-centred ferrocenium species are characterised by blue-to-green colours, it could be argued that either the thioether substituents and in particular, the relative metal coordination contribute to the nature of the HOMO levels.

Analysis of the cyclic voltammetric responses of TriMSF with scan rates varying from 0.02 to 1.00 V s^{-1} shows that: (i) in agreement with the coulometric results, the current ratio $i_{\text{pc}}/i_{\text{pa}}$ is constantly equal to 1; (ii) the current function $i_{\text{pa}}/v^{1/2}$ remains constant; (iii) the peak-to-peak separation progressively increases from 80 to 170 mV. This latter parameter indicates that the chemically reversible process is electrochemically quasi-reversible, which on a qualitative basis means that on passing from the neutral molecule to the corresponding monocation some geometrical strain must be overcome. Though not seen in Fig. 4, TriMSF also exhibits an irreversible anodic process at higher potential values (obviously assigned to the thioether substituents), which is strongly affected by electrode adsorption phenomena. In turn, complex **2** displays an irreversible two-electron reduction at very negative potential values (this is assigned to the Pt(II)/Pt(0) process).

Similar behaviour is exhibited by the ligand TMSF and its platinum complex **4**. Further supporting the assumption that the HOMO levels of these derivatives are affected by the substituents, the electrogenerated monocation of TMSF and **4** is brown in colour. The formal electrode potentials of the processes discussed above are listed in Table 3. It is interesting to note that despite the previously discussed effects on the HOMO levels, the ligands TriMSF and TMSF oxidise at the same potential values as unsubstituted ferrocene. It is also useful to emphasise the strong electron-withdrawing effect of the platinum coordination which makes the ferrocene-centred oxidation more difficult by about 0.5 V.

Table 3
Formal electrode potentials (V vs. SCE) and peak-to-peak separations (mV) for the redox processes exhibited by the ferrocene derivatives under study in dichloromethane solution

Complex	Oxidation processes				Reduction process
	$E_{1\text{st}}^{\circ}$	ΔE_p^a	$E_{2\text{nd}}^{\circ}$	ΔE_p^a	E_p^b
TRIMSF	+0.36	98	+1.31 ^{a,b}	–	–
TMSF	+0.39	84	+1.29 ^{a,b}	–	–
2	+0.91	68	–	–	–1.71 ^a
4	+0.89	67	+1.43 ^b	–	–1.61 ^a
1	+0.74	69	+1.3 ^{a,b}	–	–1.45 ^a
3	+0.73	92	+1.22 ^{a,b}	≈ 100	–1.23 ^a
FcH	+0.39	72	–	–	–

^a Measured at 0.2 V s^{-1} .

^b Peak potential for irreversible processes.

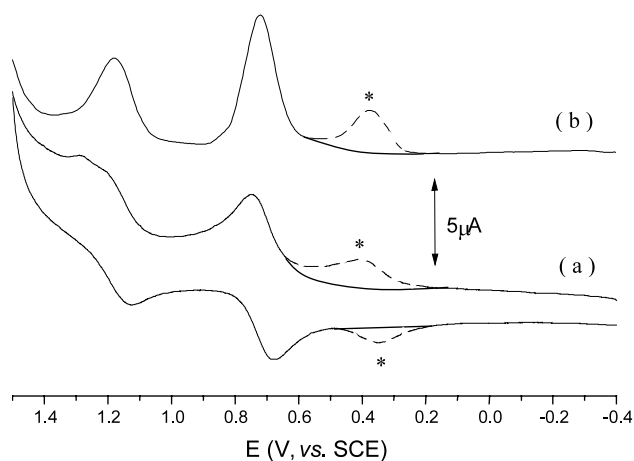


Fig. 5. Cyclic (a) and OSQW (b) voltammograms recorded at a platinum electrode on a CH_2Cl_2 solution of **3** (1.1×10^{-3} mol dm^{-3}) without (—) and with (---) the addition of a small amount of TMSF (0.2×10^{-3} mol dm^{-3}) as internal standard. $[\text{NBu}_4][\text{PF}_6]$ (0.2 mol dm^{-3}) supporting electrolyte. Scan rates: (a) 0.2 V s^{-1} ; (b) 0.1 V s^{-1} .

As illustrated in Fig. 5a, which refers to compound **3**, a slightly more complex voltammogram is exhibited by the rhenium-coordinated complexes. In fact, the anodic scan shows that the ferrocene/ferrocenium process is accompanied by a further oxidation process displaying features of chemical reversibility. Since such a process is coupled to other minor processes (we must take into account the potential redox activity of either the thioether groups or the bromide ligand, or the Re(I) moieties) and in order to understand more about the relative peak heights of the two processes, we recorded the pertinent square wave voltammogram (Fig. 5b). If allowance is made to assign such a process to the oxidation of the rhenium(I) moiety, on a purely speculative basis the OSQW voltammogram seems to rule out the concomitant oxidation of the two Re(I) centres. We note however, that **3** affords an irreversible two-electron reduction. Controlled potential coulometric tests, in analogy with the first (ferrocene-based) process, also affords the corresponding brown monocations. Attempts to measure experimentally the number of electrons involved in the most anodic step failed due to the effect of adjacent solvent discharge. Also in this case, rhenium-centred irreversible reductions are present in the cathodic region. All the relevant potential values are summarized in Table 3. As seen, the electron-withdrawing effect of the rhenium fragment(s) lowers the potential values (by about 0.15 V) with respect to that of the analogous platinum complexes.

Further work is in progress to design asymmetric multi-substituted ligands (and attach to catalytically-active metal centres) and, with the elucidation of the preferred coordination modes, to design metal-containing polymers with TMSF.

4. Experimental

4.1. General

All preparations were carried out using standard Schlenk techniques [13]. All solvents were distilled over standard drying agents under nitrogen directly before use and all reactions were carried out under an atmosphere of nitrogen. Alumina gel (neutral-grade II) was used for chromatographic separations. All NMR spectra were recorded using a Delta upgrade on a Jeol EX270 MHz spectrometer operating at 270.17 MHz (^1H) and 67.94 MHz (^{13}C - $\{^1\text{H}\}$). Chemical shifts are reported in δ using CDCl_3 (^1H , δ 7.25 ppm; ^{13}C , δ 77.0 ppm) as the reference for the spectra. Infrared spectra were recorded using NaCl solution cells (CH_2Cl_2) using a Mattson Polaris Fourier Transform IR spectrometer. Mass spectra were recorded using positive FAB methods, on an Autospec Q mass spectrometer. Microanalyses were carried out in the Department of Chemistry, University of North London. Materials and apparatus for electrochemistry have been described elsewhere [14]. All the potential values are referred to the saturated calomel electrode (SCE).

4.2. Preparation of ligands

1,1'-Bis(methylthio)ferrocene (BMSF) was prepared following a literature method [11].

4.2.1. Synthesis of 1,1',2-tris(methylthio)ferrocene (TriMSF) and 1,1',2,2'-tetrakis(methylthio)ferrocene (TMSF)

A solution of *t*-BuLi (1.7 M, 10.6 ml, 18.0 mmol) in pentane was added to BMSF (1.50 g, 9.0 mmol) in hexane (40 ml) and the reaction mixture stirred for 16 h. A light orange precipitate was formed and allowed to settle. The supernatant hexane solution was removed via cannula and freshly distilled hexane (20 ml) was added. A solution of dimethyldisulphide (1.62 ml, 18.0 mmol) in hexane (5 ml) was then added dropwise to the stirred suspension, producing a yellow precipitate after an additional 4 h stirring. Water (10 ml) was added and the reaction mixture stirred for 30 min. The organic layer was separated and the aqueous layer was extracted with hexane (2×5 ml). The combined organic extracts were dried (MgSO_4), filtered and reduced to dryness in vacuo to leave an impure foul-smelling brown oil. This was subjected to column chromatography using petroleum ether (40–60):diethylether (10:1) to elute TriMSF (1.01 g, 45%), followed by an increase in polarity of the solvent system to a 5:1 mixture to elute TMSF (0.73 g, 32%). TMSF could be obtained as a low-melting crystalline orange-brown solid after standing, coupled with rigorous removal of solvent, whilst TriMSF was isolated as a brown oil.

TriMSF: Anal. Calc. for $C_{13}H_{16}FeS_3$: C, 48.15; H, 4.94. Found: C, 47.13; H, 5.16%. 1H -NMR: δ 2.31 (s, 6H, SCH₃), 2.33 (s, 3H, SCH₃), 4.21 (br s, 2H, C₅H₄), 4.26 (br s, 1H, C₅H₃), 4.31 (br s, 2H, C₅H₄), 4.38 (br s, 2H, C₅H₃); ^{13}C - $\{^1H\}$ -NMR: δ 19.4 (SCH₃), 19.6 (SCH₃), 69.1 (C₅H₃), 71.6 (C₅H₄), 72.7 (C₅H₃), 73.0 (C₅H₄), 85.7 (C₅SR), 87.0 (C₅SR); FAB + ve m/z 324 [M]⁺ (100%), 278 [M - SCH₃]⁺ (6%).

TMSF: Anal. Calc. for $C_{14}H_{18}FeS_4$: C, 45.41; H, 4.87. Found: C, 45.28; H, 5.37%. 1H -NMR: δ 2.29 (s, 12H, SCH₃), 4.18 (t, 2H, C₅H₃, $^3J_{H-H} = 1.8$ Hz), 4.32 (d, 4H, C₅H₃, $^3J_{H-H} = 2.0$ Hz); ^{13}C - $\{^1H\}$ -NMR: δ 19.3 (SCH₃), 71.4 (C₅H₃), 74.0 (C₅H₃), 87.8 (C₅SR); FAB + ve m/z 370 [M]⁺ (24%), 324 [M - SCH₃]⁺ (3%).

4.3. Preparation of complexes

cis-PtCl₂(NCPPh)₂ [15] and Re(CO)₅Br [16] were prepared following literature procedures.

4.3.1. Synthesis of **1**

TriMSF (0.074 g, 0.20 mmol) was added to a solution of Re(CO)₅Br (0.068 g, 0.17 mmol) in THF (10 ml) and the reaction mixture stirred under reflux. The reaction was monitored by IR spectroscopy and stopped after 10 h. The reaction mixture was evaporated to dryness in vacuo to leave an oily, brown substance, which was washed with cold hexane (2 × 10 ml) to remove any unreacted ligand. The crude product was purified by two layer recrystallisation (hexane:dichloromethane—1:1) and fine orange needle-like crystals were obtained (0.094 g, 82%). Anal. Calc. for $C_{16}H_{16}FeO_3S_3Re$: C, 28.49; H, 2.39. Found: C, 28.47; H, 2.28%. 1H -NMR: δ 2.29–2.32 (br overlapping s, SCH₃), 2.80, 2.89 (br s, SCH₃), 4.18 (t, C₅H₃, $^3J_{H-H} = 1.9$ Hz), 4.23 (t, C₅H₄, $^3J_{H-H} = 1.8$ Hz), 4.26 (t, C₅H₄, $^3J_{H-H} = 1.9$ Hz), 4.35 (d, C₅H₄, $^3J_{H-H} = 2.0$ Hz), 4.52 (br t, C₅H₃), 4.80 (br d, C₅H₄); IR ν (CO) (cm⁻¹) 2037 (vs), 1948 (s br), 1906 (s br); FAB + ve m/z 674 [M]⁺ (1.5%), 646 [M - CO]⁺ (0.3%), 595 [M - Br]⁺ (5.4%), 539 [M - (CO)₂Br]⁺ (1.5%).

4.3.2. Synthesis of **2**

cis-PtCl₂(NCPPh)₂ (0.061 g, 0.13 mmol) was dissolved in toluene (65 ml) with gentle warming. A solution of TriMSF (0.051 g, 0.16 mmol) in toluene (10 ml) was added and the reaction mixture became cloudy and was then stirred at 90 °C for 15 h. The reaction volume was reduced to ca. 30 ml to produce an orange–brown precipitate. This was filtered, washed {hexane (2 × 10 ml) and diethylether (5 × 10 ml)} and the crude product was recrystallised from hexane:dichloromethane (1:1) to leave an orange–brown microcrystalline solid (0.044 g, 57%). Anal. Calc. for $C_{13}H_{16}Cl_2FeS_3Pt$: C, 26.44; H, 2.71. Found: C, 26.36; H, 2.67%. 1H -NMR: δ 2.38 (s, 3H, SCH₃) 2.85 (t, 6H, SCH₃, $^3J_{Pt-H} = 23.0$ Hz), 4.46 (t,

2H, C₅H₄, $^3J_{H-H} = 1.9$ Hz), 4.53 (t, 2H, C₅H₄, $^3J_{H-H} = 2.0$ Hz), 4.62 (d, 2H, C₅H₃, $^3J_{H-H} = 1.8$ Hz), 5.02 (t, 1H, C₅H₃, $^3J_{H-H} = 2.0$ Hz); FAB + ve m/z 590 [M]⁺ (14%), 555 [M - Cl]⁺ (40%), 519 [M - 2Cl]⁺ (2%).

4.3.3. Synthesis of **3**

A similar procedure for the formation of **1** was followed, using TMSF (0.060 g, 0.16 mmol) and Re(CO)₅Br (0.142 g, 0.35 mmol) in THF (20 ml) to form an orange–brown microcrystalline solid (0.106 g, 73%). Anal. Calc. for $C_{20}H_{18}FeO_6S_4Re_2$: C, 22.39; H, 1.88. Found: C, 22.32; H, 1.65%. 1H -NMR: δ 2.80, 2.83, 2.92, 2.93 (br s, SCH₃), 4.34 (br s, C₅H₃), 4.52 (br s, C₅H₃), 4.62, 4.63 (overlapping t, C₅H₃), 4.74, 4.90, 4.95, 5.03 (br s, C₅H₃), 5.07 (br d, C₅H₃); IR ν (CO) (cm⁻¹) 2037 (vs), 1947 (s br), 1908 (s br); FAB + ve m/z 910 [M]⁺ (8.5%), 882 [M - CO]⁺ (2.8%), 830 [M - Br]⁺ (1.8%).

4.3.4. Synthesis of **4**

A similar procedure for the formation of **2** was followed, using TMSF (0.09 g, 0.25 mmol) and *cis*-PtCl₂(PhCN)₂ (0.10 g, 0.21 mmol) in toluene (75 ml) to form an orange–brown microcrystalline solid (0.055 g, 44%). Anal. Calc. for $C_{14}H_{18}Cl_2FeS_4Pt$: C, 26.41; H, 2.83. Found: C, 26.21; H, 2.77%. 1H -NMR: δ 2.39 (s, 6H, SCH₃) 2.84 (t, 6H, SCH₃, $^3J_{Pt-H} = 23.5$ Hz), 4.47 (t, 1H, C₅H₃, $^3J_{H-H} = 2.0$ Hz), 4.58 (d, 2H, C₅H₃, $^3J_{H-H} = 1.8$ Hz), 4.61 (d, 2H, C₅H₃S₂Pt, $^3J_{H-H} = 1.9$ Hz), 4.96 (t, 1H, C₅H₃S₂Pt, $^3J_{H-H} = 1.8$ Hz); FAB + ve m/z 637 [M]⁺ (3%), 603 [M - Cl]⁺ (24%), 563 [M - 2Cl]⁺ (3%).

Crystallographic data for **1**: $C_{16}H_{16}O_3S_3BrReFe$, $M = 674.4$, monoclinic, $P2_1/n$ (no. 14), $a = 12.249(5)$, $b = 8.528(3)$, $c = 19.531(11)$ Å, $\beta = 95.83(5)^\circ$, $V = 2030(2)$ Å³, $Z = 4$, $D_{calc} = 2.207$ g cm⁻³, $\mu(Mo-K_\alpha) = 8.96$ mm⁻¹, $T = 293$ K, orange needles; 2644 independent measured reflections, F^2 refinement, $R_1 = 0.039$, $wR_2 = 0.074$, 2010 independent observed absorption corrected reflections [$|F_o| > 4\sigma(|F_o|)$, $2\theta = 45^\circ$], 239 parameters.

Crystallographic data for **3**: $C_{20}H_{18}O_6S_4Br_2Re_2Fe-CH_2Cl_2$, $M = 1155.6$, monoclinic, $P2_1/c$ (no. 14), $a = 16.547(4)$, $b = 15.008(3)$, $c = 13.851(3)$ Å, $\beta = 97.09(2)^\circ$, $V = 3413(1)$ Å³, $Z = 4$, $D_{calc} = 2.249$ g cm⁻³, $\mu(Mo-K_\alpha) = 10.27$ mm⁻¹, $T = 203$ K, yellow plates; 5453 independent measured reflections, F^2 refinement, $R_1 = 0.056$, $wR_2 = 0.134$, 3884 independent observed absorption corrected reflections [$|F_o| > 4\sigma(|F_o|)$, $2\theta = 50^\circ$], 364 parameters.

5. Supplementary material

Crystallographic data for the structural analyses have been deposited with the Cambridge Crystallographic

Data Centre, CCDC No. 162368 for compound **1**, and 162367 for compound **3**. Copies of this information may be obtained free of charge from The Director, CCDC, 12 Union Road, Cambridge CB2 1EZ, UK (fax: +44-1233-336033; e-mail: deposit@ccdc.cam.ac.uk or www: http://www.ccdc.cam.ac.uk).

Acknowledgements

This research was supported by the EPSRC via studentships to JM and CKW, and by the Department of Chemistry, Imperial College. PZ gratefully acknowledges the financial support of the University of Siena (PAR 2001).

References

- [1] (a) For a detailed literature review see: A. Togni, T. Hayashi (Eds.), *Ferrocenes: Homogeneous Catalysis–Organic Synthesis–Materials Science*, VCH, Weinheim, Germany, 1995; (b) A. Togni, R.L. Halterman (Eds.), *Metallocenes*, Wiley–VCH, Weinheim, Germany, 1998.
- [2] For a comprehensive overview of ferrocene and other metallocene chemistry see: N.J. Long, *Metallocenes: An Introduction to Sandwich Complexes*, Blackwell Science, Oxford, UK, 1998.
- [3] I.R. Butler, M.G.B. Drew, C.H. Greenwell, E. Lewis, M. Plath, S. Mussig, J. Szewczyk, *Inorg. Chem. Commun.* 2 (1999) 576.
- [4] (a) I.R. Butler, S. Mussig, M. Plath, *Inorg. Chem. Commun.* 2 (1999) 424; (b) I.R. Butler, M.G.B. Drew, *Inorg. Chem. Commun.* 2 (1999) 234; (c) I.R. Butler, R.L. Davies, *Synthesis* (1996) 1350; (d) I.R. Butler, L.J. Hobson, S.M.E. Macan, D.J. Williams, *Polyhedron* 12 (1993) 1901.
- [5] (a) R. Broussier, S. Ninoreille, C. Bourdon, O. Blacque, C. Ninoreille, M.M. Kubicki, B. Gautheron, *J. Organomet. Chem.* 561 (1998) 85; (b) R. Broussier, C. Bourdon, O. Blacque, A. Vallat, M.M. Kubicki, B. Gautheron, *J. Organomet. Chem.* 538 (1997) 83; (c) R. Broussier, S. Ninoreille, C. Legrand, B. Gautheron, *J. Organomet. Chem.* 532 (1997) 55.
- [6] (a) G.G.A. Balavoine, J.C. Daran, G. Iftime, E. Manoury, C. Moureau-Bossuet, *J. Organomet. Chem.* 567 (1998) 191; (b) G. Iftime, J.C. Daran, E. Manoury, G.G.A. Balavoine, *Organometallics* 15 (1996) 4808.
- [7] N.J. Long, J. Martin, A.J.P. White, D.J. Williams, *J. Chem. Soc. Dalton Trans.* (1997) 3038.
- [8] (a) V.C. Gibson, N.J. Long, J. Martin, G.A. Solan, J.C. Stichebury, *J. Organomet. Chem.* 590 (1999) 115; (b) N.J. Long, J. Martin, G. Opromolla, A.J.P. White, D.J. Williams, P. Zanello, *J. Chem. Soc. Dalton Trans.* (1999) 1981; (c) V.C. Gibson, N.J. Long, A.J.P. White, C.K. Williams, D.J. Williams, *Organometallics* 19 (2000) 4425; (d) V.C. Gibson, N.J. Long, A.J.P. White, C.K. Williams, D.J. Williams, *Chem. Commun.* (2000) 2359.
- [9] E.W. Abel, N.J. Long, K.G. Orrell, A.G. Osborne, V. Sik, P.A. Bates, M.B. Hursthouse, *J. Organomet. Chem.* 383 (1990) 253.
- [10] (a) E.W. Abel, N.J. Long, K.G. Orrell, A.G. Osborne, V. Sik, P.A. Bates, M.B. Hursthouse, *J. Organomet. Chem.* 394 (1990) 455; (b) E.W. Abel, N.J. Long, K.G. Orrell, A.G. Osborne, V. Sik, *J. Organomet. Chem.* 405 (1991) 375.
- [11] (a) E.W. Abel, S.K. Bhargava, K.G. Orrell, *Prog. Inorg. Chem.* 32 (1984) 1; (b) K.G. Orrell, V. Sik, D. Stephenson, *Prog. Nucl. Mag. Res. Spect.* 22 (1990) 101.
- [12] B. McCulloch, D.L. Ward, J.D. Woollins, C.H. Brubaker Jr, *Organometallics* 4 (1985) 1425.
- [13] R.J. Errington, *Advanced Practical Inorganic and Metalorganic Chemistry*, Blackie, London, 1997.
- [14] F. Fabrizi de Biani, F. Laschi, P. Zanello, G. Ferguson, J. Trotter, G.M. O’Riordan, T.R. Spalding, *J. Chem. Soc. Dalton Trans.* (2001) 1520.
- [15] T. Uchiyama, Y. Toshiyasu, Y. Nakamura, T. Miwa, S. Kawaguchi, *Bull. Chem. Soc. Jpn.* 54 (1981) 181.
- [16] S.B. Schmidt, W.C. Trogler, F. Basolo, *Inorg. Synth.* 23 (1985) 44.